HHS Public Access

Author manuscript

Cytometry B Clin Cytom. Author manuscript; available in PMC 2019 November 01.

Published in final edited form as:

Cytometry B Clin Cytom. 2018 November ; 94(6): 941–945. doi:10.1002/cyto.b.21545.

High-Dimensional Single Cell Mapping of Cerium Distribution in the Lung Immune Microenvironment of an Active Smoker

Adeeb H. Rahman[1,2,3,*], **Yonit Lavin**[2], **Soma Kobayashi**[2], **Andrew Leader**[2], and **Miriam Merad**[2,3,4]

[1]Department of Genetics and Genomic Sciences, Icahn School of Medicine at Mt. Sinai, New York 10029

[2]Icahn School of Medicine at Mt. Sinai, The Precision Immunology Institute, New York 10029

[3]Icahn School of Medicine at Mt. Sinai, Human Immune Monitoring Center, New York 10029

[4]Department of Oncological Sciences, Icahn School of Medicine at Mt. Sinai, New York 10029

Abstract

Background—Mass cytometry leverages inductively coupled mass spectrometry to perform high dimensional single cell analyses using antibodies tagged with rare earth isotopes that are considered to be largely absent in biological samples. We have recently noted an unusual exception to this rule while analyzing tissue samples from patients undergoing surgical resection for early stage lung cancer, and here we present a detailed cytometric characterization of cerium in a clinical patient sample.

Methods—We performed a CyTOF analysis on cell suspensions derived from matched blood, tumor lesion, and non-involved lung tissue from an active smoker undergoing surgical resection for early stage lung adenocarcinoma. The samples were stained with a 31-parameter antibody panel to allow a detailed characterization of the cellular heterogeneity of the samples. The data were visualized using viSNE, major immune subsets were identified based on canonical marker expression patterns, and single cell cerium levels were evaluated across each of these defined subsets.

Results—High dimensional immune cell mapping revealed that high levels of cerium were specifically associated with a phenotypically distinct subset of lung macrophages that were most prevalent in noninvolved lung tissue, whereas tumor associated macrophages showed relatively lower levels of cerium. We hypothesize that these findings reflect alveolar macrophage phagocytosis of inhaled cerium derived from cigarette flint lighters.

Conclusions—These results demonstrate the first high-dimensional single cell characterization of environmental metal exposure associated with smoking, and offer a demonstration of the unique potential for applying mass cytometry to the field of environmental toxicology.

Correspondence to: Dr. Adeeb Rahman, Department of Genetics and Genomic Sciences, Icahn School of Medicine at Mt. Sinai, 1470 Madison Ave., New York 10029, USA. adeeb.rahman@mssm.edu.

Conflict of interest: The authors have no conflicts of interest to disclose

Additional supporting information may be found in the online version of this article at the publisher's web-site

Key terms

CyTOF; lung; cerium; microenvironment; mass cytometry; macrophage; cancer; immune monitoring; immunophenotyping; immunology

Cytometry by time-of-flight mass spectrometry (CyTOF) is a powerful cytometric technique that is analogous to conventional fluorescence flow cytometry, but instead employs metal isotope-tagged antibodies and inductively coupled mass spectrometry to measure single cell protein expression (1). By overcoming the limitations of fluorescence spectral overlap, CyTOF allows the simultaneous measurement of a much greater number of parameters with minimal spillover. One of the core principles of CyTOF is that the lanthanide isotopes that are typically analyzed on the instrument are largely absent in biological samples, and consequently any signals that are detected can be associated specifically with the labeling reagents used in the experiment.

Current CyTOF instruments have 135 detection channels in the mass range from 75 to 209 atomic mass units, and up to 40 of these channels are typically used to detect isotopically labeled antibodies and other cell-labeling reagents such as DNA intercalators, viability stains, or membrane stains (2). In addition to detecting metal-labeled cells, CyTOF experiments typically incorporate bead controls that are spiked into samples to track and normalize for possible fluctuations in instrument performance (3). Commercial EQ Four Element Calibration Beads (Fluidigm) are polystyrene beads labeled with known amounts of natural abundance cerium, europium, holmium, and lutetium. Of these elements, Ce140, the dominant isotope of cerium, is generally not used to label cells for CyTOF analyses, and consequently the Ce140 + DNA− calibration beads can be readily distinguished from Ce140-DNA+ cells during analysis. In this study, we present a case report highlighting an unusual exception to this rule, showing high levels of cerium in a clinical patient sample.

We have recently conducted a detailed multi-scale characterization of the lung and tumor immune microenvironment in patients with early stage lung cancer, including CyTOF analyses of cell suspensions derived from resected adenocarcinoma lesions and adjacent non-involved lung tissues (4). In analyzing the data from these patients, we noted unusually high levels of cell-associated cerium in some samples, and in this case report we present a detailed CyTOF characterization of single-cell cerium distribution across immune subsets in one patient who was an active smoker, identifying specific accumulation of cerium in a subset of lung macrophages.

MATERIALS AND METHODS

The detailed materials, methods, and results from the broader study characterizing the immune microenvironment of early stage lung cancer have been previously reported (4).

Patient Specimens

Blood, noninvolved lung, and tumor tissues were obtained from 15 patients with lung adenocarcinoma undergoing wedge resection or lobectomy at the Mount Sinai Medical Center (New York) after obtaining informed consent. All protocols were reviewed and

approved by the Institutional Review Board (IRB) at the Icahn School of Medicine at Mount Sinai (IRB 08–1236). The patient specifically highlighted in this report was a 71 year-old Caucasian male subject who was an active smoker with a smoking history of 75 pack-years diagnosed with moderately differentiated papillary adenocarcinoma.

Sample Collection and Processing

Samples were processed as previously described (4). Briefly, tissue samples were collected from the surgical resection specimen at the site of the tumor lesion and a second non-involved site as distant as possible from the tumor. The samples were minced with scissors, followed by enzymatic digestion with complete media supplemented with 0.225 mg/ml collagense IV (Sigma) for 45 min at 70°C. The tissues were then dissociated into single cell suspensions by passing through a 16-gauge needle and filtering through a 70 μm cell strainer, and red blood cells were lysed using RBC lysing buffer (Biolegend). Peripheral blood samples were collected intraoperatively into sodium heparin vacutainers, and peripheral blood mononuclear cell (PBMC) were isolated using Ficoll-Paque PLUS (GE Healthcare).

Equivalent cell suspensions from each tissue (blood, tumor, and noninvolved lung) were barcoded by labeling with CD45-antibodies conjugated to distinct metal isotopes, and then pooled and stained for viability with 5 μM cisplatin (5) in PBS (Fluidigm) for 2 min at RT (Supporting Information Table S1, highlighted in blue). Cells were then washed and stained with a panel of 31 antibodies designed to comprehensively characterize lung immune populations, particularly myeloid cell subsets (Supporting Information Table S1), and incubated for 30 min on ice. The samples were then washed, fixed, and permeabilized (eBiosciences) at 4°C overnight before being stained with intracellular antibodies (Supporting Information Table S1, highlighted in yellow). They were washed and incubated in 0.125 nM Ir intercalator (Fluidigm) diluted in PBS containing 2% formaldehyde, and stored at 4°C until acquisition.

CyTOF Data Acquisition

Immediately prior to acquisition, samples were washed once with PBS, washed once with deionized water, and then resuspended at a concentration of 1 million cells/ml in deionized water containing a 1:20 dilution of EQ 4 Element Beads (Fluidigm). The samples were acquired on a CyTOF2 (Fluidigm) equipped with a SuperSampler fluidics system (Victorian Airships) at an event rate of <500 events/s. After acquisition, the data were normalized using bead-based normalization in the CyTOF software and uploaded to Cytobank (6) for analysis.

Data Analysis and Visualization

CD45 barcodes were deconvolved by manual Boolean gating to separate cells from each tissue, and the data were gated to exclude residual normalization beads, debris, dead cells and doublets, leaving DNA +CD45 + $Cisplatin^{low}$ events for subsequent clustering and high dimensional analyses. Data from the three tissues were analyzed using viSNE (7), a dimensionality reduction algorithm that allows visualization of multidimensional data in two dimensional space (channels used to determine tSNE dimensions are indicated in Supporting Information Table S1). Major immune populations were identified and gated on the viSNE

map on the basis of canonical marker expression patterns. Median marker expression levels for each population were also visualized using heat-maps scaled to each marker. The relative frequency of each defined population in each tissue was exported and plotted using Graphpad Prism.

RESULTS

In performing detailed CyTOF analyses on a series of blood, tumor, and noninvolved lung samples from patients with early stage lung cancer, we noted unusually high levels of cell-associated Ce140 signal in some patient samples, particularly in one patient who was an active smoker with a smoking history of 75 pack-years (highlighted in red in Fig. 1A).

To better characterize the unusual cerium signal in the samples from this patient, we employed viSNE analyses to visualize the high dimensional cytometry data from viable CD45+ cells in matched PBMCs, tumor, and noninvolved lung tissue. Overlaying Ce140 signal intensity onto these viSNE maps showed that the Ce140 signal was largely localized to a specific subset of cells that was most prevalent in noninvolved lung tissue and largely absent from the blood (Fig. 1B). We next manually gated and identified 11 major immune subsets on the viSNE map on the basis of canonical marker expression patterns (Fig. 1C, D), revealing that the cells expressing the highest levels of Ce140 were a specific subset of macrophages, which we designate “Macrophage 1,” that expressed high levels of several markers including HLA-DR, CD64, CD163, and CD206. While the median Ce140 intensity was generally high in the Macrophage 1 population, we noted significant heterogeneity of Ce140 signal at the single cell level, and also observed generally lower Ce140 signal intensity levels in the tumor than the noninvolved lung when comparing the phenotypically analogous Macrophage 1 population across both tissues (Fig. 1E, top row: Tumor Ce140 IQR = 26.15–392.14; Lung Ce140 IQR = 40.52–782.22). Notably, this specific subset of macrophages was also more prevalent in normal lung tissue (Fig. 1F), suggesting that they represent tissue-resident alveolar lung macrophages. A second, phenotypically distinct subset of macrophages, “Macrophage 2,” was more abundant in the tumor lesion (Fig. 1F), and likely represents tumor-associated macrophages. While the Macrophage 2 subset also expressed elevated levels of Ce140 relative to other immune populations, the median intensity within this population was an order of magnitude lower than in the Macrophage 1 subset. Overall, these data demonstrate high levels of cerium specifically localized to a phenotypically distinct subset of lung resident macrophages.

DISCUSSION

It is already well established that environmental contaminants may serve as potential sources of non-specific signals that can interfere with mass cytometry experiments. Some of these contaminants may be inadvertently introduced during sample processing, such as barium, which is often found in commercial detergents, or mercury, which can be present in reagents that use thimerosal as a preservative. In addition, certain clinical treatments may also contribute to high levels of background contamination, such as platinum-containing chemotherapeutic agents (8) and gadolinium contrast agents (9). In this report, we demonstrate for the first time that residues associated with smoking may also contribute to

metal signals that are detectable by CyTOF. By leveraging the high-dimensional analytical capabilities of mass cytometry, we were able to accurately map the single cell distribution of these environmental metal contaminants and localize them to a specific subset of lung macrophages.

Previous studies have examined the potential for accumulation of metals derived from tobacco and cigarette smoke in the lungs of smokers, including cadmium and lead (10,11), which we have also observed in lung macrophages from some patients (data not shown), however cerium is generally not considered to be abundant in tobacco products. Furthermore, while we observed high levels of cerium in lung macrophages from some smokers, this was not universally the case for all smokers, and did not appear to directly correlate with overall cigarette smoke exposure as measured by pack-years, suggesting that cigarette smoke itself may not be the source of the cerium observed in this study. While we have not definitively determined the source, we hypothesize that it derives from the use of flint lighters, which often use ferrocerium or “mischmetal” alloys (12). In support of this hypothesis, the elevated levels of Ce140 in lung macrophages were also associated with elevated levels of La139 (data not shown), which is consistent with the metal composition of these alloys, which are typically comprised of a ~2:1 ratio of cerium and lanthanum. Thus, igniting a cigarette lighter and inhaling the resulting dust particles provides a plausible source for these metal ions in lung samples. The specific level of accumulation in an individual smoker may be influenced by several factors including the overall exposure, the specific kind of cigarette lighter, the proximity and inhalation behavior while lighting a cigarette, or even the phagocytic attributes of a patient’s specific macrophages.

Alveolar macrophages play a critical role in clearing pathogens and particles from the alveolar surface, providing an explanation for why cerium was found to specifically localize to this population of cells in the patient samples highlighted in this report and in all other lung tissue samples where we have observed elevated levels of cerium (Fig. 1A and data not shown). Smokers are known to have an accumulation of alveolar macrophages in their lungs, and several reports have demonstrated functional abnormalities in lung macrophages associated with smoking (13,14). Inhalation exposure to cerium oxide nanoparticles has been shown to induce pulmonary toxicity in rodent models (15,16); however, it remains unclear whether accumulation of cerium, lanthanum, or other metals in lung macrophages may directly contribute to functional dysregulations or to the development of lung cancer in patients; the findings presented here offer an avenue for further investigation of these questions. In contrast with alveolar macrophages, tumor-associated macrophages would be expected to have less exposure to the alveolar surface based on their tissue localization, which is consistent with the lower levels of cerium that we observe in these macrophages. Given that lung tumor lesions contain a phenotypically and functionally heterogeneous mixture of macrophages and that we have yet to establish markers to conclusively stratify these populations, it is intriguing to consider that differences in environmental metal exposure may offer an additional means to distinguish tissue resident macrophages from newly recruited tissue-infiltrating macrophages in tumors and other inflammatory lesions.

Overall, these results offer the first high dimensional single cell characterization of environmental metal exposure in patient tissue samples, demonstrating the specific

accumulation of cerium in alveolar macrophages from an active smoker. This study also highlights the unique capabilities of mass cytometry in the field of environmental toxicology, and the novel application of high resolution single-cell monitoring of environmental metal exposure.

Supplementary Material

Refer to Web version on PubMed Central for supplementary material.

Acknowledgments

Grant sponsor: NIH; Grant number: S10 OD023547-01.

The authors thank Oksana Mayovska, Xinzheng Guo and the Human Immune Monitoring Center for CyTOF support. They also thank Mike Leipold and Christoph Schwarzler for their insightful discussions and contributions on CyTOF Forum on a wide range of topics including mass cytometry background contamination.

LITERATURE CITED

1. Bandura DR, Baranov VI, Ornatsky OI, Antonov A, Kinach R, Lou X, Pavlov S, Vorobiev S, Dick JE, Tanner SD. Mass cytometry: technique for real time single cell multitarget immunoassay based on inductively coupled plasma time-of-flight mass spectrometry. Anal Chem. 2009; 81:6813–6822. [PubMed: 19601617]
2. Stern AD, Rahman AH, Birtwistle MR. Cell size assays for mass cytometry. Cytometry Part A. 2017; 91A:14–24.
3. Finck R, Simonds EF, Jager A, Krishnaswamy S, Sachs K, Fantl W, Pe'er D, Nolan GP, Bendall SC. Normalization of mass cytometry data with bead standards. Cytometry Part A. 2013; 83A:483–494.
4. Lavin Y, Kobayashi S, Leader A, Amir ED, Elefant N, Bigenwald C, Remark R, Sweeney R, Becker CD, Levine JH, et al. Innate Immune Landscape in Early Lung Adenocarcinoma by Paired Single-Cell Analyses. Cell. 2017; 169:750–765. [PubMed: 28475900]
5. Fienberg HG, Simonds EF, Fantl WJ, Nolan GP, Bodenmiller B. A platinum-based covalent viability reagent for single-cell mass cytometry. Cytometry Part A. 2012; 81A:467–475.
6. Kotecha N, Krutzik PO, Irish JM. Web-based analysis and publication of flow cytometry experiments. Curr Protoc Cytom. 2010; Chapter 10(Unit10.17)
7. Amir ED, Davis KL, Tadmor MD, Simonds EF, Levine JH, Bendall SC, Shenfeld DK, Krishnaswamy S, Nolan GP, Pe'er D. viSNE enables visualization of high dimensional single-cell data and reveals phenotypic heterogeneity of leukemia. Nat Biotechnol. 2013; 31:545–552. [PubMed: 23685480]
8. Fricker SP. Metal based drugs: From serendipity to design. Dalton Trans. 2007:4903–4917. [PubMed: 17992275]
9. Chevrier S, Levine JH, Zanotelli VRT, Silina K, Schulz D, Bacac M, Ries CH, Ailles L, Jewett MAS, Moch H, et al. An Immune Atlas of Clear Cell Renal Cell Carcinoma. Cell. 2017; 169:736–749. [PubMed: 28475899]
10. Ashraf MW. Levels of Heavy Metals in Popular Cigarette Brands and Exposure to These Metals via Smoking. Sci World J. 2012; 2012:e729430.
11. Pinto E, Cruz M, Ramos P, Santos A, Almeida A. Metals transfer from tobacco to cigarette smoke: Evidences in smokers' lung tissue. J Hazard Mater. 2017; 325:31–35. [PubMed: 27914289]
12. Reinhardt K, Winkler H. Cerium Mischmetal, Cerium Alloys, and Cerium Compounds. Ullmann's Encylopedia of Industrial Chemistry. 2000
13. Wallace WA, Gillooly M, Lamb D. Intra-alveolar macrophage numbers in current smokers and non-smokers: A morphometric study of tissue sections. Thorax. 1992; 47:437–440. [PubMed: 1496503]

14. Monick MM, Powers LS, Walters K, Lovan N, Zhang M, Gerke A, Hansdottir S, Hunninghake GW. Identification of an autophagy defect in smokers' alveolar macrophages. J Immunol. 2010; 185:5425–5435. [PubMed: 20921532]

15. Nemmar A, Yuvaraju P, Beegam S, Fahim MA, Ali BH. Cerium Oxide Nanoparticles in Lung Acutely Induce Oxidative Stress, Inflammation, and DNA Damage in Various Organs of Mice. Oxid Med Cell Longev. 2017; 2017:9639035. [PubMed: 28392888]

16. Rice KM, Nalabotu SK, Manne NDPK, Kolli MB, Nandyala G, Arvapalli R, Ma JY, Blough ER. Exposure to Cerium Oxide Nanoparticles Is Associated With Activation of Mitogen-activated Protein Kinases Signaling and Apoptosis in Rat Lungs. J Prev Med Pub Health. 2015; 48:132–141. [PubMed: 26081650]

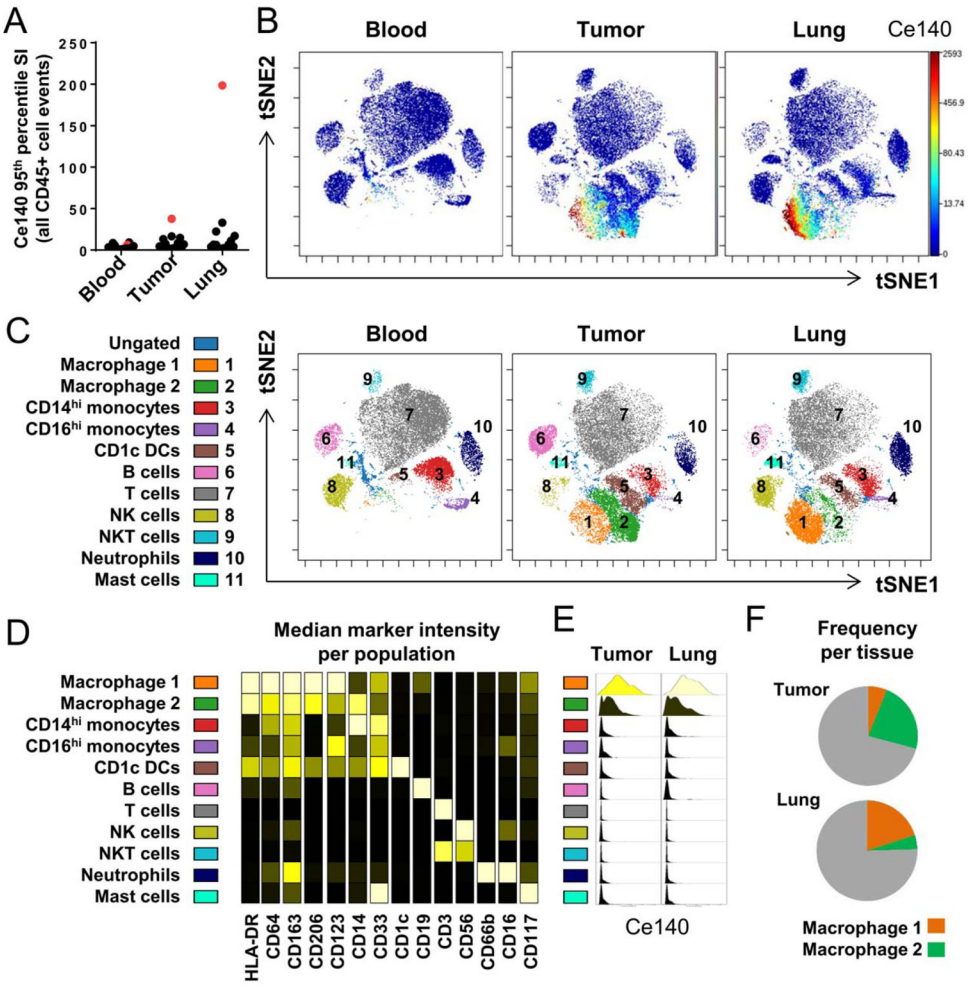

Fig. 1.

Paired blood, tumor, and noninvolved lung tissue collected from surgical resection specimens were processed and analyzed by CyTOF. **A**: 95th percentile Ce140 signal intensity for all DNA+ CD45 gated cell events (*n* = paired samples from 15 patients; the patient with unusually high Ce140 levels is highlighted in red and analyzed further in **B**–**F**). B: Paired viSNE analysis showing single-cell Ce140 signal intensity levels in blood, tumor, and noninvolved lung samples from the highlighted patient. C: Major immune populations were manually gated and identified on the viSNE map on the basis of canonical marker expression patterns, as summarized in (D). Each column on the heatmap is scaled independently to show relative expression of that parameter across all populations (dark = low expression; light = high expression). E: Histograms showing single-cell Ce140 signal intensity within each of the defined immune populations from the tumor and noninvolved lung tissue. Histogram shading denotes median Ce140 signal intensity, scaled across all histograms. F: Relative frequency of each of the macrophage populations as a percentage of total viable CD45+ cells in each of the tissues.